NAVAL POSTGRADUATE SCHOOL
Monterey, California

AD-A258 055

DTIC
ELECTE
DEC 17 1992
S A D

THESIS

X-RAY DIFFRACTION AND ELECTRON MICROSCOPE
STUDIES OF YTTRIA STABILIZED ZIRCONIA (YSZ)
CERAMIC COATINGS EXPOSED TO VANADIA

by

Kostandinos G. Kondos

September, 1992

Thesis Advisor: Alan G. Fox

Approved for public release; distribution is unlimited.

92-31678

REPORT DOCUMENTATION PAGE

1a. REPORT SECURITY CLASSIFICATION Unclassified	1b. RESTRICTIVE MARKINGS
2a. SECURITY CLASSIFICATION AUTHORITY	3. DISTRIBUTION/AVAILABILITY OF REPORT Approved for public release; distribution is unlimited.
2b. DECLASSIFICATION/DOWNGRADING SCHEDULE	

4. PERFORMING ORGANIZATION REPORT NUMBER(S)	5. MONITORING ORGANIZATION REPORT NUMBER(S)

6a. NAME OF PERFORMING ORGANIZATION Naval Postgraduate School	6b. OFFICE SYMBOL (If applicable) 34	7a. NAME OF MONITORING ORGANIZATION Naval Postgraduate School
6c. ADDRESS (City, State, and ZIP Code) Monterey, CA 93943-5000		7b. ADDRESS (City, State, and ZIP Code) Monterey, CA 93943-5000

8a. NAME OF FUNDING/SPONSORING ORGANIZATION	8b. OFFICE SYMBOL (If applicable)	9. PROCUREMENT INSTRUMENT IDENTIFICATION NUMBER

8c. ADDRESS (City, State, and ZIP Code)	10. SOURCE OF FUNDING NUMBERS			
	Program Element No.	Project No.	Task No.	Work Unit Accession Number

11. TITLE (Include Security Classification)

X-RAY DIFFRACTION AND ELECTRON MICROSCOPE STUDIES OF
  YTTRIA STABILIZED ZIRCONIA (YSZ) CERAMIC COATINGS EXPOSED TO VANADIA

12. PERSONAL AUTHOR(S) Konstandinos G. Keados

13a. TYPE OF REPORT Master's Thesis	13b. TIME COVERED From To	14. DATE OF REPORT (year, month, day) September, 1992	15. PAGE COUNT 52

16. SUPPLEMENTARY NOTATION
The views expressed in this thesis are those of the author and do not reflect the official policy or position of the Department of Defense or the U.S. Government.

17. COSATI CODES			18. SUBJECT TERMS (continue on reverse if necessary and identify by block number)
FIELD	GROUP	SUBGROUP	Ceramic, Zirconia, YSZ, Vanadia, Degrades, XRD, TEM, SEM, EDX

19. ABSTRACT (continue on reverse if necessary and identify by block number)

The U.S. Navy sometimes has the requirement to use low cost fuels containing significant amounts of vanadium and sulfur in gas turbine engines. Unfortunately the yttria stabilized zirconia (YSZ) witch is used as a thermal barrier coating on gas turbine blades can be severely attacked by vanadia. Powders of YSZ containing 8-mol% Y_2O_3 and pure zirconia containing various amounts of V_2O_5 were annealed at 900 C. These were then examined by X-ray diffraction and electrom microscopy, as well as single crystals of pure ZrO_2 and YSZ (20% wt Y_2O_3) exposed to V_2O_5 melts, to study how the vanadium degrades the YSZ by reacting with the stabilizer to form YVO_4 and how the vanadia transforms the cubic and tetragonal YSZ crystal structures to monoclinic which degrades rapidly as a gas turbine blade coating.

20. DISTRIBUTION/AVAILABILITY OF ABSTRACT ☒ UNCLASSIFIED/UNLIMITED ☐ SAME AS REPORT ☐ DTIC USERS	21. ABSTRACT SECURITY CLASSIFICATION Unclassified	
22a. NAME OF RESPONSIBLE INDIVIDUAL Alan G. Fox	22b. TELEPHONE (Include Area code) (408) 663-3275	22c. OFFICE SYMBOL ME/Fx

DD FORM 1473, 84 MAR   83 APR edition may be used until exhausted   SECURITY CLASSIFICATION OF THIS PAGE
All other editions are obsolete   Unclassified

X-ray Diffraction and Electron Microscope
Studies of Yttria Stabilized Zirconia (YSZ)
Ceramic Coatings Exposed to Vanadia

by

Konstandinos G. Kondos
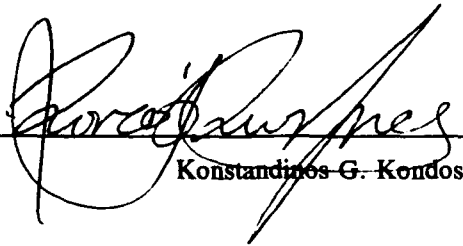Lieutenant J.G., Hellenic Navy
B.S., Hellenic Naval Academy, 1985

Submitted in partial fulfillment
of the requirements for the degree of
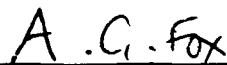
MASTER OF SCIENCE IN MECHANICAL ENGINEERING

from the

NAVAL POSTGRADUATE SCHOOL
September 1992

Author: _____
Konstandinos G. Kondos

Approved by: _____
A .Ci .Fox
Alan G. Fox, Thesis Advisor

_____
Matthew D. Kelleher, Chairman
Department of Mechanical Engineering

ii

ABSTRACT

The U.S. Navy sometimes has the requirement to use low cost fuels containing significant amounts of vanadium and sulfur in gas turbine engines. Unfortunately the yttria stabilized zirconia (YSZ) which is used as a thermal barrier coating on gas turbine blades can be severely attacked by vanadia. Powders of YSZ containing 8-mol% Y_2O_3 and pure zirconia containing various amounts of V_2O_5 were annealed at 900°C. These were then examined by X-ray diffraction and electron microscopy, as well as single crystals of pure ZrO_2 and YSZ (20%wt Y_2O_3) exposed to V_2O_5 melts, to study how the vanadium degrades the YSZ by reacting with the stabilizer to form YVO_4 and how the vanadia transforms the cubic and tetragonal YSZ crystal structures to monoclinic which degrades rapidly as a gas turbine blade coating.

iii

TABLE OF CONTENTS

LIST OF TABLES

LIST OF FIGURES

ACKNOWLEDGEMENTS

I would like to express my sincere appreciation and gratitude to my advisor Alan G. Fox for his assistance and guidance and without whom I would not have completed this thesis.

I dedicate this thesis to my wife, Kalliopi, and my two sons, Georgios and Andreas, for their great help, support, and encouragement during all my time at NPS, including late nights and weekends that were spent in writing this thesis. Finally a special thanks is due to the Hellenic Navy for giving me this special opportunity to study at the Naval Postgraduate School.

I. INTRODUCTION

Yttria-stabilized zirconia has been developed for use as a thermal barrier coating on hot section gas turbine blades, which, by allowing higher gas temperature, can increase engine efficiency by 10% or more.

Unfortunately using these coatings with cheap fuels, particularly those containing vanadium and sulfur has led to dramatically reduced coating lifetimes. There have been several suggestions as for the origin of this degradation, in particular the $ZrO_2 \bullet Y_2O_3$-V system has been intensively studied using various methods for varying the activity of V in the neighborhood of the YSZ. As a result of these experiments some workers suggest that degradation of the YSZ arises as a result of preferential diffusion of Y_2O_3 out of the YSZ to react with V_2O_5 to form YVO_4 leaving a monoclinic solid solution behind which rapidly degrades [Ref.2] [Ref.18]. On the other hand Patton et al [Ref.10] suggest that vanadium can interact with cubic/tetragonal YSZ without yttria depletion to form a monoclinic ternary solid solution which also degrades quicly.

In the present work attempts will be made to try and understand the true nature of the reaction between V and YSZ.

II. BACKGROUND

A. CRYSTALLOGRAPHY OF ZIRCONIA

1. Cubic

The cubic phase has a fluorite-type crystal structure, in which each Zr is coordinated by eight equidistant oxygens and each oxygen is tetrahedrally coordinated by four zirconiums and it is stable from 2370 °C to the melting point (2680 ± 15 °C). [Ref.1], [Ref.2]
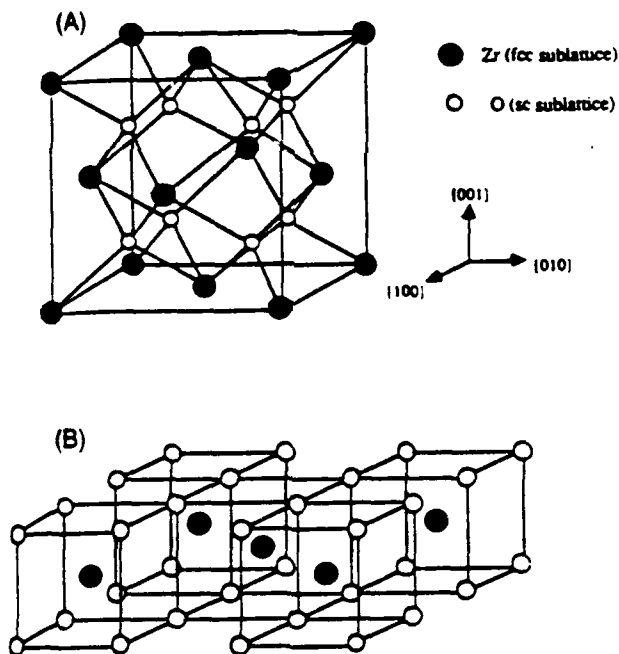
Figure 1. Schematic diagrams of fluorite structure of cubic ZrO_2 emphasizing (A) face-centered cubic packing of cation sublattice and (B) simple-cubic packing of anion sublattice. [Ref.2:p.1001]

2. Tetragonal

In this phase the Zr is surrounded by eight oxygens, four at a distance of 0.2465 nm and the other four at a distance of 0.2065 nm ; the phase is stable between about 1170°C and 2370°C. [Ref.1]

3. Monoclinic

This phase is stable at all temperatures below 1170°C and the coordination of Zr is sevenfold which suggests a certain degree of covalency as well as ionicity in the bonding. [Ref.1]

B. PHASE TRANSFORMATIONS OF ZIRCONIA

Zirconia exhibits the following transformations: [Ref.2]

monoclinic $\rightleftharpoons^{1170°C}$ tetragonal $\rightleftharpoons^{2370°C}$ cubic $\rightleftharpoons^{2680°C}$ liquid

1. Monoclinic ⇌ Tetragonal

This transformation was first detected by Ruff and Ebert in 1929 using high temperature XRD [Ref.1]. Wolten was the first to suggest that this transformation is martensitic; the forward transition of this transformation occurs at 1170°C and the reverse one at 950°C. The transformation T→M is accompanied by a 3-5% volume increase which causes stresses and failure to zirconia ceramic coatings. The crystal structures of tetragonal and monoclinic zirconia are shown in Figure 2 [Ref.3:p.96]. [Ref.1], [Ref.2], [Ref.3]

3

MONOCLINIC
a_m = 0.51881 nm
b_m = 0.52142 nm
c_m = 0.53835 nm
β = 81.22

TETRAGONAL
a_t = 0.51485 nm
b_t = 0.52692 nm
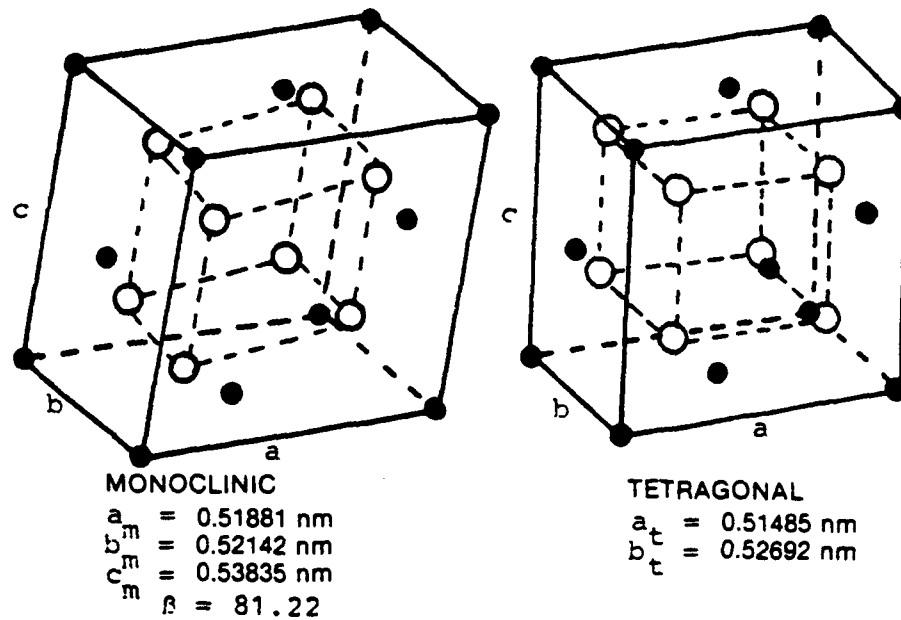
Figure 2. Crystal structures of monoclinic and tetragonal zirconia with lattice parameters at 950°C for both phases.

2. Tetragonal → Cubic

This displacive transformation is diffusionles, composition-invariant but, as noted [Ref.6], and occurs with a change in crystal symmetry relative to the parent cubic phase. The transformation is also accompanied by the formation of twins, especially in polycrystalline materials.[Ref.6]

C. PHASE DIAGRAMS OF ZIRCONIA BINARY SYSTEMS

The zirconia-yttria system, shown in figure 3, is one of the most interesting zirconia binary systems because of the relatively large cubic solid solution field. The diagram indicates that the greater the content of yttria the more stable the cubic phase. A mixture of cubic and monoclinic (or

4

tetragonal) zirconia occurs when the yttria is present in a concentration less than that needed for complete stabilization of cubic fluorite-type zirconia phase) or when the fully stabilized, cubic zirconia with a suitable solute content is heat-treated under appropriate conditions of temperature and time. [Ref.1], [Ref.5]
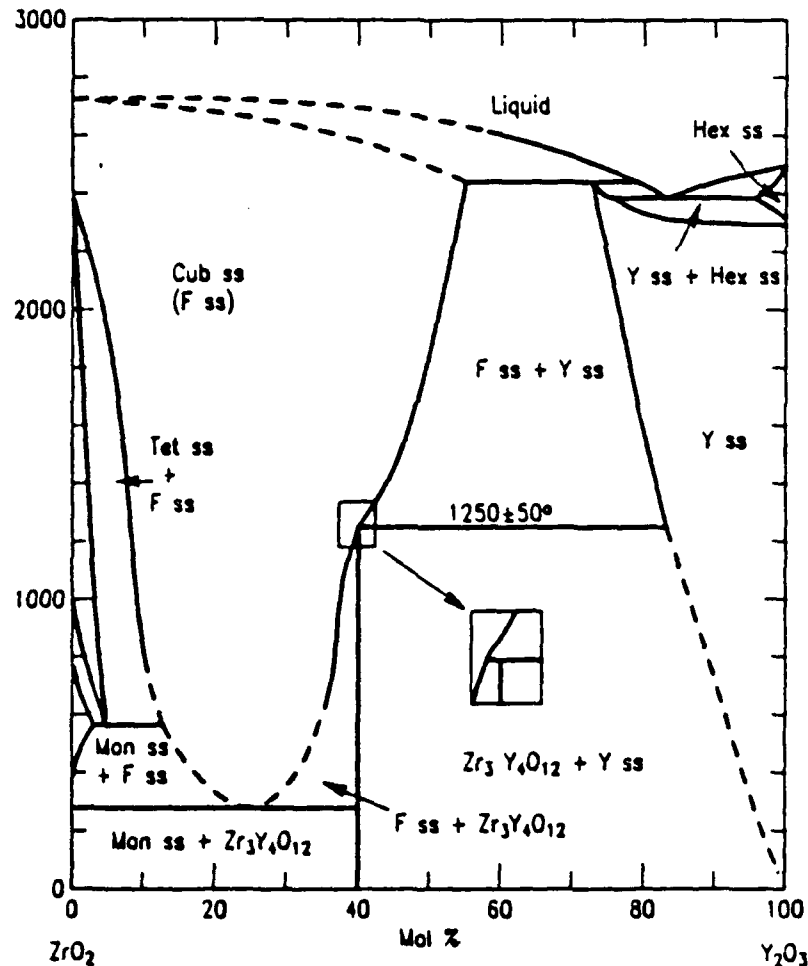
Figure 3. System ZrO_2-Y_2O_3. F = fluorite type of ZrO_2; Y = Y_2O_3; Cub = cubic; Tet = tetragonal; Mon = monoclinic; Hex = hexagonal. [Ref.4]

There are several other oxides that used to form a solid solution with zirconia, like CaO, MgO, Sc_2O_3, CeO_2, In_2O_3 etc., because they have a relatively high solubility in zirconia (see for example [Ref.16],[Ref.17]) and are able to form fluorite-type phases with ZrO_2 which are stable over wide ranges of composition and temperature. Two of the commonly used stabilizers for zirconia thermal barrier coatings are magnesia and calcia; their binary phase diagrams with zirconia are shown below in figure 4 [Ref.11], and figure 5 [Ref.5] respectively.
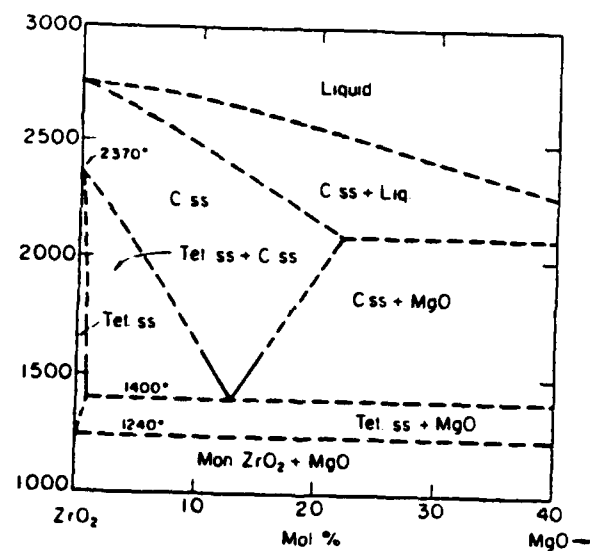
Figure 4. System ZrO_2-MgO showing ZrO_2-rich side.
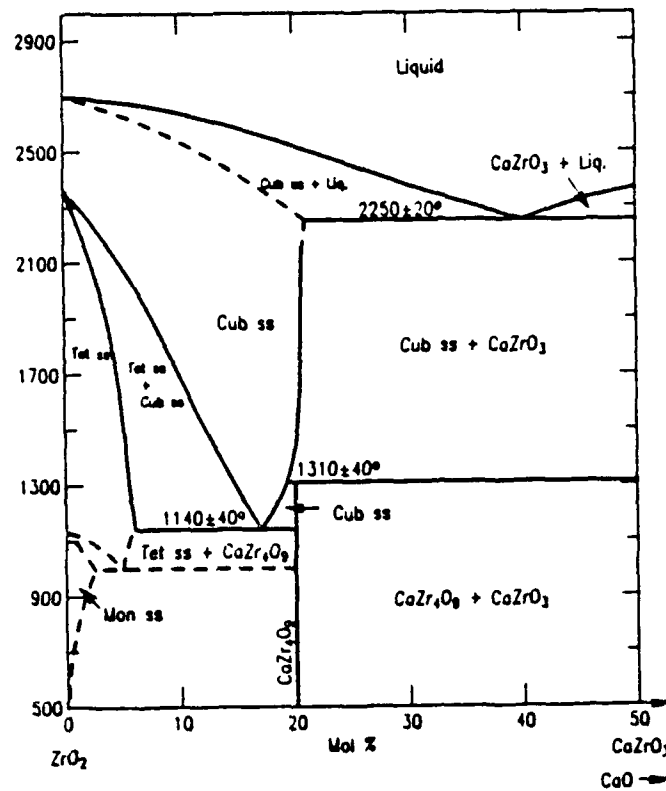
Figure 5. Zirconia-calcia binary system.

D. MECHANICAL PROPERTIES OF ZIRCONIA

Table I.[Ref.1:p.14] shows that the coexistence of tetragonal and cubic zirconia results in strength and fracture toughness values approximately three times those of a mixture of monoclinic and cubic phases or only cubic zirconia.

TABLE I. STRENGTH AND FRACTURE TOUGHNESS OF ZIRCONIA

	Transverse rupture strength (MPa)	K_{IC} ($MN/m^{3/2}$)
Tetragonal + cubic ZrO_2	650	≈7.1
Monoclinic + cubic ZrO_2 (overaged at 1400°C)	250	3.7
Cubic ZrO_2 (solution annealed at 1850°C, 4 h)	245	2.8

E. DESTABILIZATION OF YSZ BY CHEMICAL ATTACK

The destabilization of YSZ, thermal barrier coatings in gas turbine engines, is caused by the vanadium and sulfur high level contaminants in low quality fuels.

1. Reaction of Vanadium Compounds with Ceramic Oxides

Some reactions of vanadium compounds with ceramic oxides, and products, are collected in Figure 6. [Ref.7:p.228] The reactions are mainly driven by the Lewis acid-base mechanism type where, acids react with bases, but not acids with acids or bases with bases. [Ref.8]

	Na$_3$VO$_4$	NaVO$_3$	V$_2$O$_5$
Y$_2$O$_3$	NR	YVO$_4$	YVO$_4$
CeO$_2$	NR	NR	CeVO$_4$
ZrO$_2$	NR	NR	ZrV$_2$O$_7$ (BUT SLOWLY)
GeO$_2$	Na$_4$Ge$_9$O$_{20}$	Na$_4$Ge$_9$O$_{20}$[*]	NR
Ta$_2$O$_5$	NaTaO$_3$	Na$_2$Ta$_4$O$_{11}$	α-TaVO$_5$

(left vertical axis label: INCREASING ACIDITY)

NR = NO REACTION
[*] AS PPT FROM H$_2$O SOL'N

Figure 6. Reaction behavior and products of ceramic oxides with vanadium compounds.

2. Reaction of V$_2$O$_5$ with ZrO$_2$
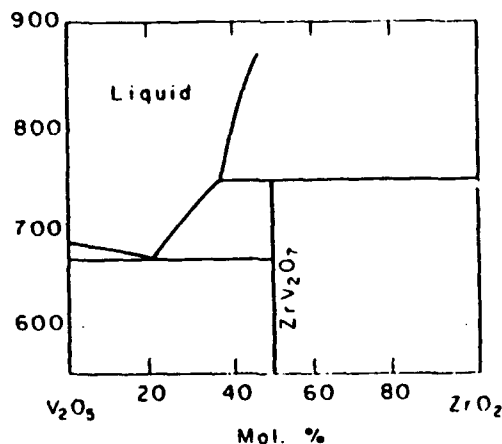
Figure 7. System V$_2$O$_5$-ZrO$_2$

The phase diagram of ZrO$_2$-V$_2$O$_5$ system shown in figure 7 [Ref.13], suggests that for low V$_2$O$_5$ contents the reaction product will be (monoclinic) ZrO$_2$ + (cubic) ZrV$_2$O$_7$ since

in the composition ranges of interest the amount of V_2O_5 is small. The reaction can be written as follows.

$$ZrO_2 + V_2O_5 = ZrV_2O_7 \qquad (1)$$
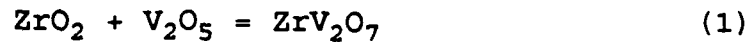
However, the phase diagram of V-O system, shown in figure 8 [Ref.15], does not show what phase is stable, V_2O_5 or V_2O_4, at 900°C which is the working temperature for the gas turbines, and the temperature of interest in the present work.
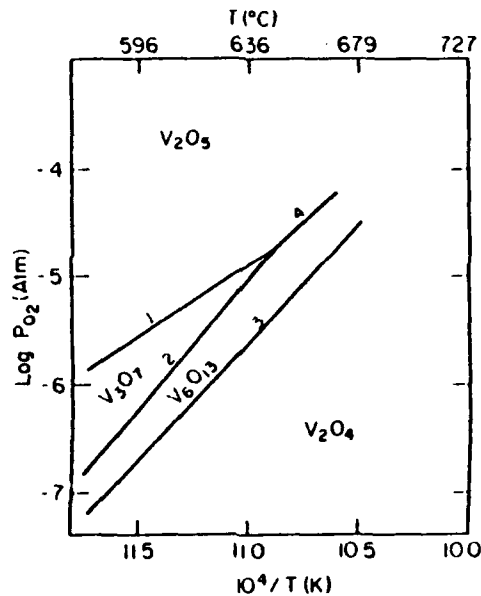
Figure 8. System V-O

This figure 8 suggests by extrapolation that V_2O_4 is stable at 900°C; this is also suggested by the Y_2O_3-V_2O_5 phase diagram (figure 9), where the V-rich phases are shown to be deficient in oxygen.

3. Reaction of V_2O_5 with Y_2O_3

The phase diagram of Y_2O_3-V_2O_5 system is shown in figure 9 [Ref.14]. All the reactions which have been considered between V_2O_5 and Y_2O_3 in the present work lead to the formation of YVO_4 which suggests that V_2O_5 and Y_2O_3 react on an equimolar basis, thus

$$V_2O_5 + Y_2O_3 = 2YVO_4 \qquad (2)$$
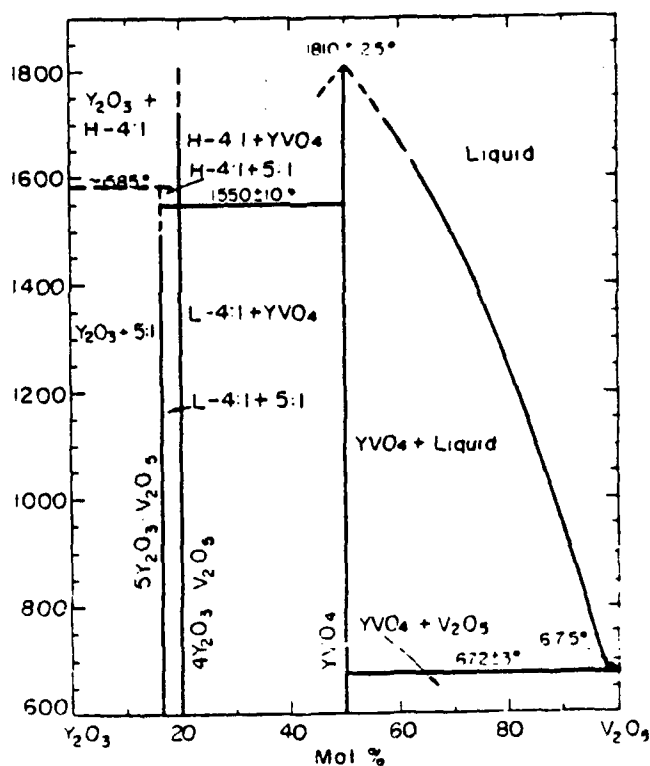
Figure 9. System Y_2O_3-V_2O_5. The Y_2O_3-YVO_4 subsystem is probably pseudobinary because of oxygen losses from the 4:1 and 5:1 phases. L and H = low and high forms, respectively.

11

4. Reactions of YSZ with Vanadium Pentoxide

The reaction (2) of the Y_2O_3 stabilizer in YSZ matrix, with the V_2O_5 component of the molten contaminant deposits can be rewritten as follows.

$$Y_2O_3 \ (\text{ in } ZrO_2 \ ) + V_2O_5 \ (\text{ in melt }) =$$
$$2YVO_4 \ (\text{ solid precipitate }) \tag{3}$$

$$Y_2O_3 \ (\text{ base }) + V_2O_5 \ (\text{ acid }) = 2YVO_4 \ (\text{ salt }) \tag{3a}$$

$$Y_2O_3 \ (\ a<1 \ ) + V_2O_5 \ (\ a<1 \ ) = 2YVO_4 \ (\ s,a=1 \ ) \tag{3b}$$
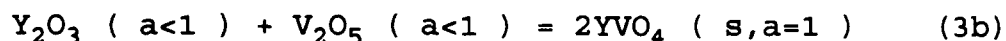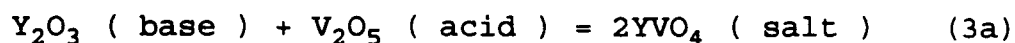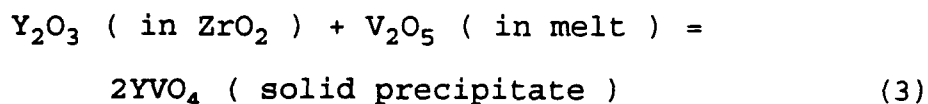
The reaction (3) is rewritten as (3a) to emphasize the Lewis acid-base nature, and as (3b) to emphasize that the activities of yttrium oxide in YSZ and vanadium pentoxide in melt are less than one ($a<1$), and the YVO_4 is considered to form as a pure solid with activity equal to one ($s,a=1$) [Ref.9]. The formation of yttrium vanadate from this reaction leaches the Y_2O_3 from solid solution in the zirconia matrix, and causes destabilization from the tetragonal (or cubic) to monoclinic structure of zirconia. [Ref.10]

Another reaction which could take place is between ZrO_2 and V_2O_5 to form ZrV_2O_7. This is extraordinarily slow as discussed in [Ref.7]; it is certainly slower than the reaction of V_2O_5 with Y_2O_3.

The recent results of Patton et al [Ref.10], in which a single crystal YSZ was exposed to V_2O_5 melts at 900°C for 100 hours are presented in figure 10 [Ref.10:p.8].

12
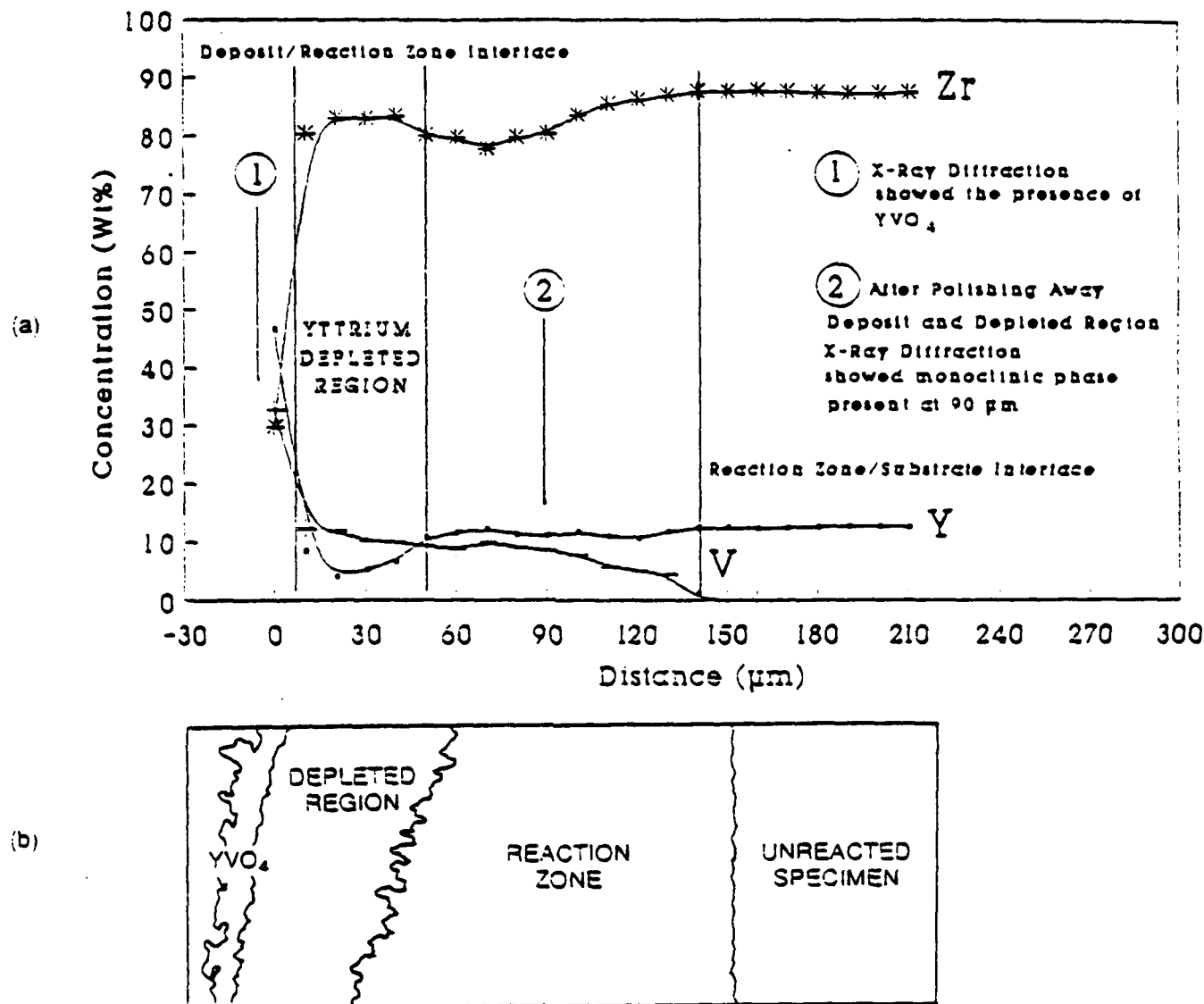
Figure 10. (a) Concentration variations for yttrium, vanadium and zirconium existing in a YSZ specimen after 100 hours compared to (b) a schematic illustrating the orientation of the different regions of the specimen.

These results show that in the outer region, near the surface, the yttrium was depleted by the vanadium to form

13

YVO_4; but at greater depths where significant amounts of vanadium was detected, no YVO_4 could be found nor was there depletion of Y_2O_3; in this region the presence of the monoclinic phase was shown by XRD. This suggests that perhaps it is not necessary to generate YVO_4 for the vanadium to degrade the YSZ, and that at low vanadium activities the YSZ could be degraded without the formation of YVO_4.

F. SCOPE OF PRESENT WORK

From previous research and literature presented here some important conclusions can be drawn:

- ZrO_2 reacts with V_2O_5 slowly to form ZrV_2O_7 [Ref.7]; there is no evidence of a monoclinic solid solution of V_2O_4, which is possible at 900°C, or V_2O_5 in ZrO_2.

- Y_2O_3 reacts on an equimolar basis with V_2O_5 to form YVO_4 which is always found on the surface of YSZ coatings exposed to vanadium. [Ref.2]

- V_2O_5 (maybe V_2O_4) can react with YSZ to form what appears to be a ternary monoclinic solid solution [Ref.10], and Patton (private communication) has suggested that with very low V activities a monoclinic ternary solid solution of ZrO_2-Y_2O_3-V_2O_5 (maybe V_2O_4) can form without the presence of YVO_4.

The present work will involve X-ray diffraction (XRD), scanning electron microscopy (SEM), and transmission electron microscopy (TEM) studies of the following:

- The true reaction of V_2O_5 with ZrO_2 at 900°C in air to see if there is formation of a solid solution, using both powders and single crystal specimens.

- Reinvestigation of the reaction between powdered V_2O_5 and ZrO_2-8mol%Y_2O_3 in air at 900°C to try and further understand the degradation of YSZ with V, since the exact mechanism (or mechanisms) of V_2O_5 attack is still unclear.

III. EXPERIMENTAL PROCEDURE

A. SAMPLE PREPARATION

1. Powder Samples

Fine powders of YSZ (TZ-8Y, ZrO_2-8mol% Y_2O_3) and pure zirconia (TZ-0, ZrO_2), were provided by Tosoh Inc., as well as vanadium pentoxide (V_2O_5) typically 99.9% pure by J.T. Baker Chemical Co.

An accurate balance (Sartorius-Werke AG) was used to make powder mixtures of YSZ with 1, 3, 5, 7, and 10 weight percent of V_2O_5 as well as mixtures of ZrO_2 with 2, 5, and 10 weight percent of V_2O_5. All the powder mixtures were reacted at 900°C for 168 hours.

2. Single Crystal Sample

A specimen of a single crystal of YSZ (ZrO_2 + 20%wt Y_2O_3) ,as well as of pure ZrO_2, was supplied by Dr J.Patton, Naval Surface Warfare Center, Annapolis MD; the specimen was exposed to V_2O_5 melts at 900°C in air for 50 hours. The activity of the V_2O_5 was maintained at 5.2×10^{-5}. The specimen was cut transverse to the exposed surface and cold mounted in epoxy resin. This was then coated in carbon to make it conducting for the SEM.

B. X-RAY DIFFRACTION

The powder samples described above were passed through a U.S. standard #400 sieve mesh ($38\mu m$) and then mounted into a specimen holder by using acetone to wet the powder. A razor blade were used to remove the excess powder on the sample holder and make a flat surface. The final step consisted of using a final layer of acetone to settle and clean the residual powder around the holder.

X-ray diffraction was performed using a Phillips PW1700 X-ray Diffractometer (XRD) with a copper target (Cu alpha 1, 2 wavelengths = 1.54060, 1.54439 Å), equipped with a Philips microprocessor controller. A power setting of 30kV, 35mA and a scan rate of 2 seconds running for a step 0.05 degrees (0.025 deg/s) was suitable for collecting all the raw data.

The raw data was analyzed by using a VAX 3100 workstation and the peak positions and integrated intensities were determined and recorded using Phillips APD1700 software which curve fits each individual peak.

C. TRANSMISSION ELECTRON MICROSCOPY (TEM)

Powder samples were crushed and then collected on a 400 mesh copper grids, coated with a thin layer of carbon.

A JEOL 100 TEM, with voltage setting 120kV,was used to investigate the samples. Photographs were taken of bright field images and diffraction patterns.

D. SCANNING ELECTRON MICROSCOPY (SEM)

The powder samples of the reacted mixtures were passed through a U.S. standard #400 sieve mesh over an SEM sample holder covered with a thin layer of conducting adhesive. The microstructures were then studied in a Cambridge, Model S200 SEM equipped with a Kevex x-ray energy dispersive spectrometer (EDX). The chemical analysis was also measured by EDX to check for loss of components during the heat treatment.

The SEM backscattered imaging method was used on the single crystal sample to examine the phases present in the reacted zone and in the unreacted specimen. It was determined that backscattered image provided improved detection of the phases present in the reacted zone using atomic number contrast [Ref.19:p.149].

IV. RESULTS AND DISCUSSION

A. XRD RESULTS

1. ZrO_2 - V_2O_5

a. Unreacted in the Mechanically Mixed State

The XRD results of the unreacted powder samples of pure ZrO_2 with 2, 5, and 10 weight percent V_2O_5 show the monoclinic ZrO_2 peaks and the orthorhombic V_2O_5 peaks as expected. Figure 11(a) shows the raw data of the 5% sample with V_2O_5 and ZrO_2 peaks.

b. Annealed at 900°C

After annealing the samples at 900°C , 2 and 5% for 72 hours, and the 10% for 168 hours, there was no evidence of the cubic ZrV_2O_7 or the V_2O_5 peaks. Figure 11(b) shows the raw data of the 5% sample with only monoclinic ZrO_2.

TABLE II. ZrO_2-V_2O_5 REACTED INTENSITIES

ZrO_2 ($\bar{1}11$) M peak Intensity(counts)	V_2O_5 in ZrO_2 (weight %)	Reaction time at 900°C (hours)
9053	2	72
8047	5	72
6742	10	168
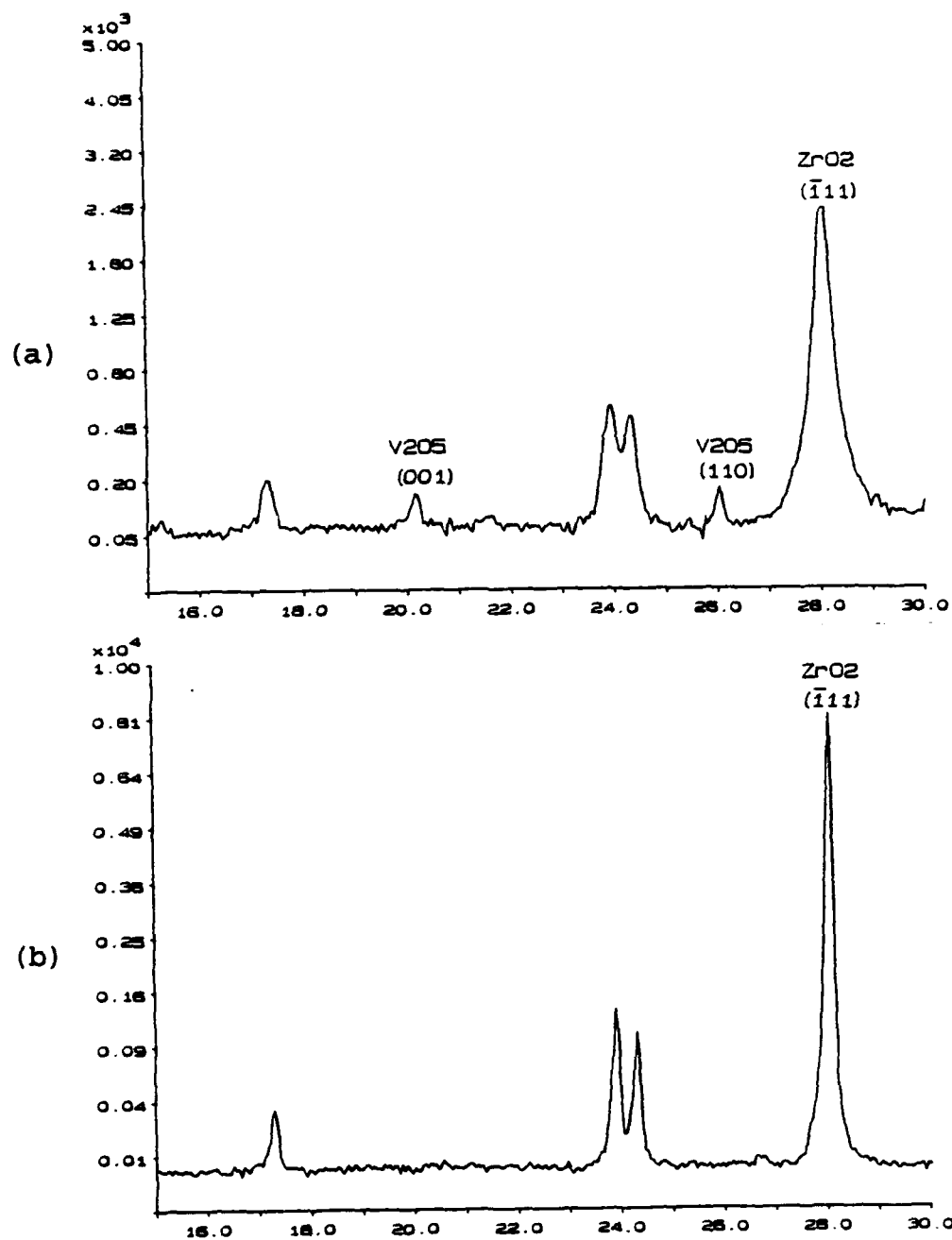
Figure 11. XRD raw data of ZrO_2-5%wt V_2O_5:
(a) unreacted, (b) reacted.

20

Table ii summarizes the intensities of the ($\bar{1}11$) monoclinic (M) peak for all the reacted samples. The table shows that increasing the amount of V_2O_5 causes the ($\bar{1}11$) M peak to go down; there are two possible reasons which could explain this reduction; these are:

● some V_2O_5 reacts with ZrO_2 to form a glassy phase,

● or the V_2O_5 reacts with ZrO_2 to form a solid solution.

Thermodynamic calculations and the V-O phase diagram [Ref.15] pose the question; has the V_2O_5 (V valency 5) been transformed to VO_2 (V valency 4) which is more likely to dissolve in the ZrO_2 matrix, which has also been suggested by Matkovich et al [Ref.20]. The increase in reaction time from 3 to 7 days it doesn't seem to make any difference to this reaction which confirms all previous work on this topic [Ref.7] [Ref.12] and suggests that the reaction is extremely slow.

c. ZrO_2 Single Crystal

The results of the pure ZrO_2 monoclinic single crystal close to [$\bar{2}15$] zone axis, exposed to V_2O_5 vapor at 900°C for 50 hours, showed no sign of V_2O_5 or ZrV_2O_7. The XRD pattern was found to contain monoclinic peaks only.

2. YSZ with V_2O_5 Annealed at 900°C

The results of the ZrO_2-8mol% Y_2O_3, with 1, 3, 5, 7, and 10 percent weight of V_2O_5, powder samples reacted at 900°C for 168 hours, and 100 hours (10% sample only), show that YVO_4 (Y) is definitely formed by the reaction (3), as well as the transformation of cubic/tetragonal (C) YSZ to monoclinic (M) ZrO_2. Table iii summarizes the higher intensities of the C (111), M ($\bar{1}$11), and Y (200) peaks for the various reacted samples.

TABLE III. SELECTED PEAK INTENSITIES OF YSZ-V_2O_5 REACTED SAMPLES

V_2O_5 %wt	(111) C, Peak (counts)	($\bar{1}$11) M, Peak (counts)	(200) Y, Peak (counts)	Reaction time (hours)
1	11485	643	350	168
3	8878	1591	729	168
5	7044	1949	1262	168
7	2964	5004	1995	168
10	0	6982	2601	100

Table iii shows that by increasing the amount of V_2O_5, the formation of tetragonal YVO_4 increases, as well as monoclinic ZrO_2. Figure 12 shows a comparison of the XRD raw data between the 1%, figure 12(a), and the 10% sample, figure 12(b), to emphasize the growth of the YVO_4 and ZrO_2 at the

expense of the cubic/tetragonal YSZ phase. Figure 13 is a plot of the C, M, and Y percentages present versus the weight percentage of the V_2O_5 reacted with YSZ at 900°C. The points derived by the relationship, % reaction product = 100*X/(C+M+Y) (where X = C, M, or Y).

The nonlinearity of the C and M curves leads to the conclusion that for higher amounts than 5% V_2O_5 the destabilization of YSZ is more rapid without being affected much by the almost linear growth of YVO_4 or the time of reaction. It can be seen that only 100 hours was adequate for the complete destabilization of the YSZ-10%wt V_2O_5 sample.
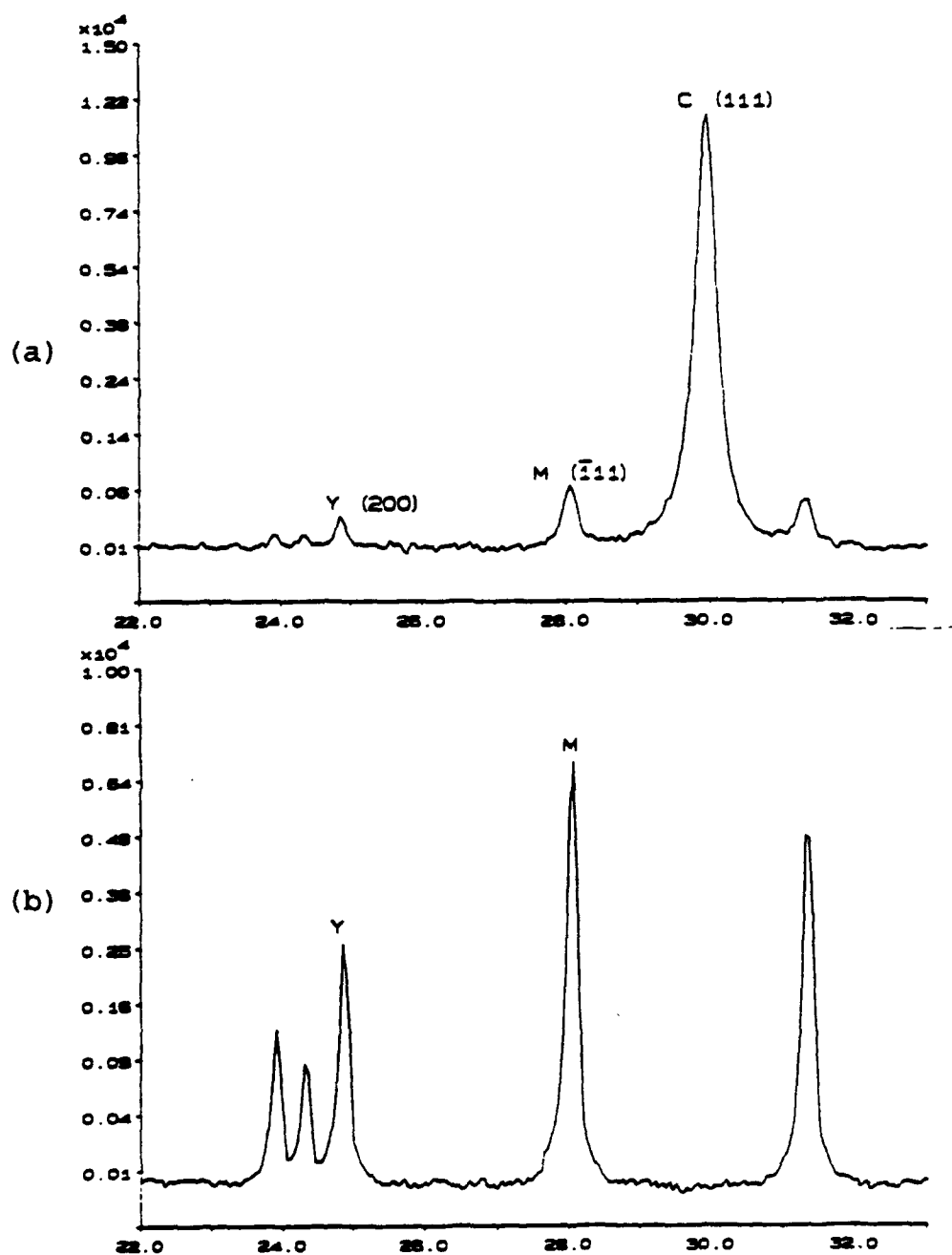
Figure 12. XRD raw data of reacted samples:
(a) YSZ-1%wt V_2O_5 and (b) YSZ-10%wt V_2O_5

24

DESTABILIZATION OF YSZ
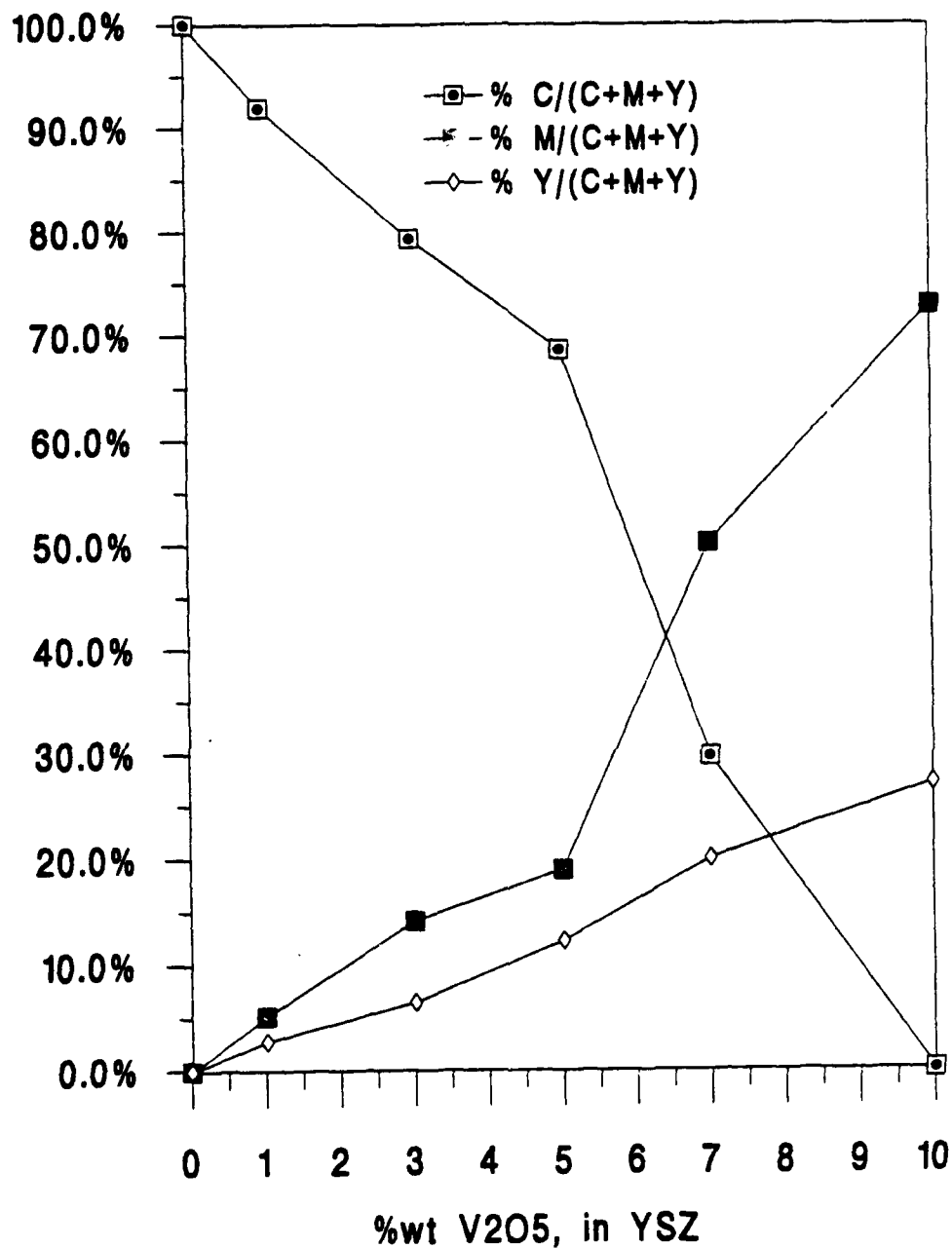
Figure 13. Plot of C, M, Y% content vs %wt of V_2O_5 in YSZ powder samples annealed at 900°C.

B. TEM RESULTS

It was very difficult to get thin single phase regions from the TEM powder samples, thus it was not possible to get good diffraction patterns.

1. ZrO_2-5%wt V_2O_5

A TEM powder sample of the ZrO_2-5%wt V_2O_5 reacted at 900°C for 72 hours was examined. Particles were usually overlapped and not thin enough for diffraction and accurate EDX analysis and gave a wide range of compositions. Two bright field micrographs were taken of particles shown in figures 14, and 15, as well as the EDX chemical analysis. Table iv shows the oxide percentage of the two particles.

TABLE IV. EDX ANALYSIS OF ZrO_2-5% V_2O_5 PARTICLES

Element & Line	Oxide % Figure 14	Oxide % Figure 15
V Kα	3.96	42.69
Zr Lα	96.04	57.31

These analyses, on table iv, show some evidence of ZrV_2O_7 composition, for example the particle in figure 15, which was not seen in the XRD results, on the other hand there may be some glassy phases associated ZrO_2+V_2O_5 reaction, which would not detected by XRD. Further TEM investigations should

26

be performed on single crystals of pure ZrO_2 exposed to V_2O_5 corrosion environment vapors for much longer periods of time since it is known that the reaction takes place very slowly.

Figure 14. ZrO_2-5%wt V_2O_5 reacted at 900°C for 72 hours, particle oxide percent composition close to overall composition. Bright field TEM micrograph.

84 nm

Figure 15. ZrO_2-5%wt V_2O_5 reacted at 900°C for 72 hours, particle oxide percent composition close to fifty-fifty (atomic). Bright field TEM micrograph.

2. YSZ with V_2O_5 Annealed at 900°C

TEM powder samples of the YSZ-1% V_2O_5 reacted at 900°C for 168 hours and YSZ-10% V_2O_5 reacted at 900°C for 100 hours were examined. Particles were again overlapped and were usually not thin enough for diffraction and accurate EDX analysis and gave a wide range of compositions. Three bright field micrographs were taken of particles shown in figures

28

16(a), 16(b), and 17, as well as the EDX chemical analysis. Table v shows the oxide percentage of the three particles.

TABLE V. EDX ANALYSIS OF YSZ-V_2O_5 REACTED PARTICLES

Element & Line	Oxide % Figure 16(a)	Oxide % Figure 16(b)	Oxide % Figure 17
V Kα	31.25	2.54	92.15
Y Lα	54.35	17.93	4.99
Zr Lα	14.4	79.53	2.86

These analyses, in table v, reconfirm the existence of YVO_4 as expected, in the particle shown in figure 16(a), evidence of which was also seen in the XRD results. On the other hand the existence of almost pure ZrO_2 monoclinic phase with a touch of YVO_4 is demonstrated from an analysis of the particle in figure 16(b). In addition, unreacted V_2O_5 with a touch of YVO_4 plus monoclinic ZrO_2 was detected in the particle shown in figure 17. This suggests that not all the Y_2O_3 (in ZrO_2) reacts with the V_2O_5 to form YVO_4, but perhaps some of the V_2O_5 reacts with the ZrO_2 to form a glassy phase or a solid solution. Further TEM experiments should be performed on single crystals of YSZ exposed to V_2O_5 corrosion environment vapors, to investigate the phases present in the reacted zone.
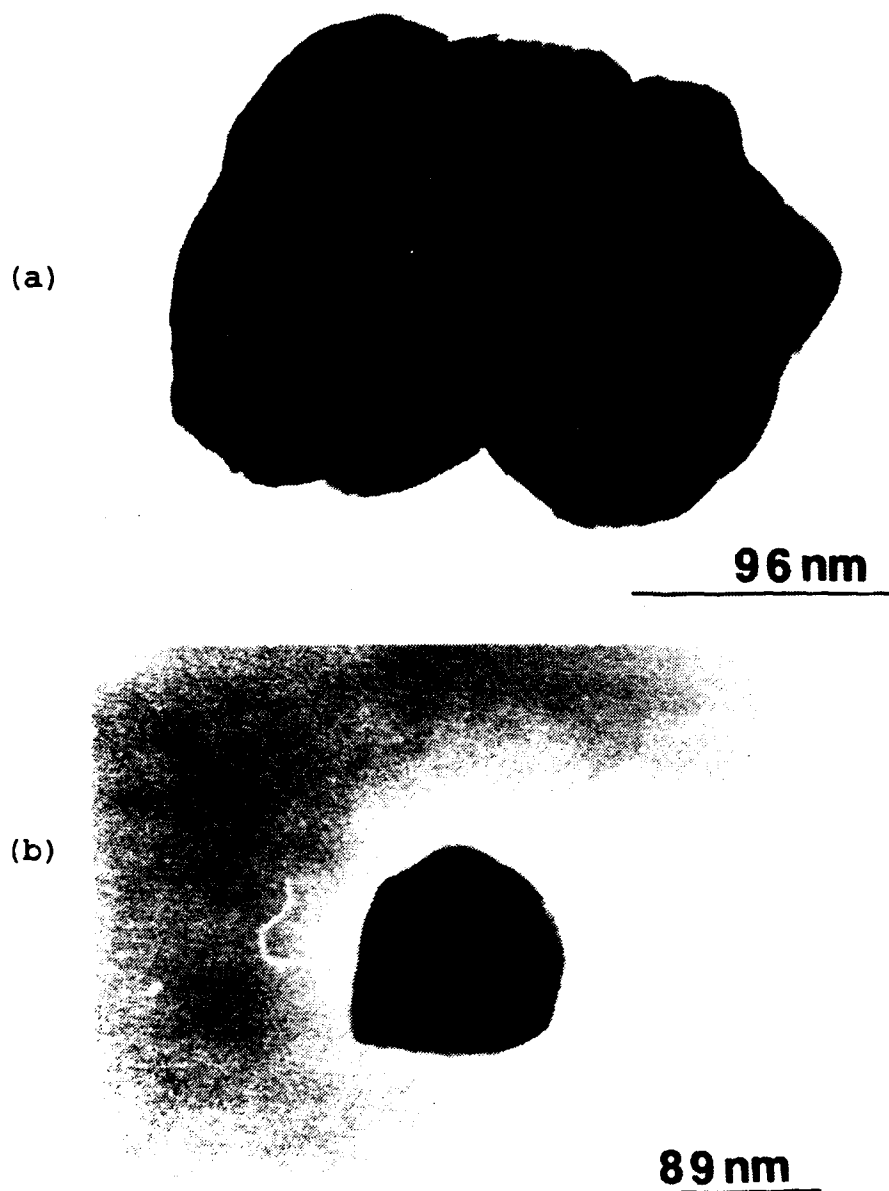
(a)

96 nm

(b)

89 nm

Figure 16. YSZ-1%wt V_2O_5 reacted at 900°C for 168 hours. **(a)** The particle composition mostly YVO_4 with a touch of ZrO_2. **(b)** Particle with composition mostly ZrO_2 with a touch of YVO_4. Bright field TEM micrographs.

30

56 nm

Figure 17. YSZ-10%wt V_2O_5 reacted at 900°C for 100 hours. The particle composition shows unreacted V_2O_5 with a touch of YVO_4 and ZrO_2. Bright field TEM micrograph.

C. SEM RESULTS

1. ZrO_2-5%wt V_2O_5 Powder Reacted at 900°C

Only the overall chemical analysis performed by EDX was useful, for the ZrO_2-5%wt V_2O_5 powder sample reacted at 900°C for 72 hours, which confirmed no loss of the components V or Zr.

2. Single Crystal of YSZ Exposed to V_2O_5

Single crystal of YSZ (20 wt% Y_2O_3) exposed to V_2O_5 melts at 900°C in air for 50 hours was examined by SEM. The activity of V_2O_5 was maintained at 5.2×10^{-5}. The specimen was

cut transverse to the exposed surface and examined across the reaction zone. Table vi summarizes the chemical analysis across the reaction zone. At the beginning of the reaction zone region marked with an arrow as shown in figure 18, the light phase (10 μm across) appears to be pure ZrO_2 by EDX analysis.
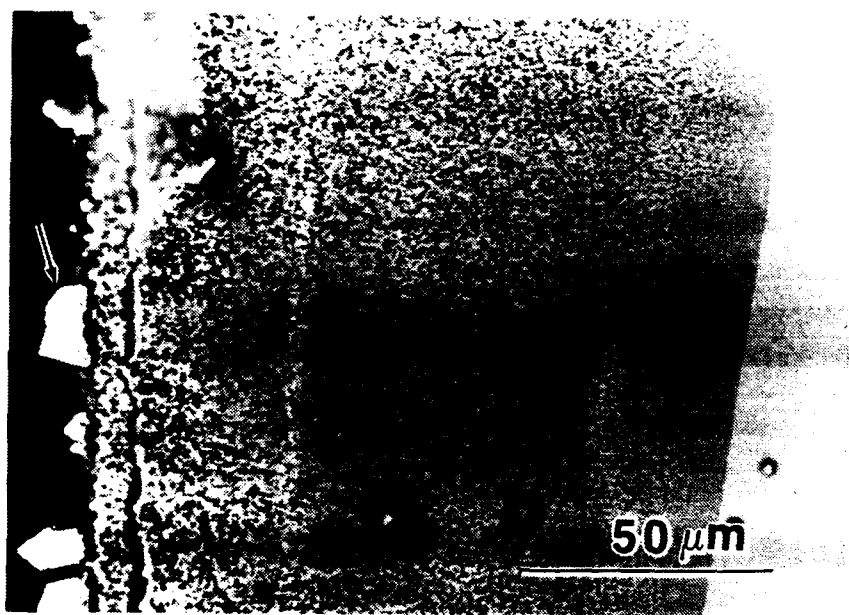

Figure 18. YSZ (20 wt% Y_2O_3) single crystal sample: Exposed to V_2O_5 vapors at 900°C in air for 50 hours. Activity of V_2O_5 was maintained at 5.2 x 10^{-5}. Backscattered SEM micrograph showing the reaction zone. Atomic number contrast clearly shows segregation into two regions, one V-rich and one V-deficient.

32

TABLE VI. EDX ANALYSIS OF YSZ SINGLE CRYSTAL EXPOSED TO V_2O_5

Examined Area	Element Zr	Element V	Element Y	
Figure 18 particle as marked	99.35	0.65	0.0	wt%
Figure 19 Dark region near start of zone	22.9	31.61	46.10	wt%
	17.66	37.48	44.86	at%
Figure 20 Light region near center of reaction zone	84.68	8.11	7.21	wt%
	79.43	13.63	6.94	at%
Figure 20 Dark region near center of reaction zone	41.84	22.61	35.55	wt%
	35.22	34.07	30.71	at%
Figure 21 End of reaction zone overall	79.10	9.34	11.56	wt%
	73.46	15.52	11.02	at%
YSZ Matrix composition	80.6	0.0	19.4	wt%

The dark phase that is shown in figure 19 (2 μm wide) in the beginning of the reaction zone is mostly YVO_4 as showed by EDX analysis. The presence of ZrO_2 may be from the

neighboring white phase area, since the probing area was close
to the limit of resolution of x-ray analysis mode.
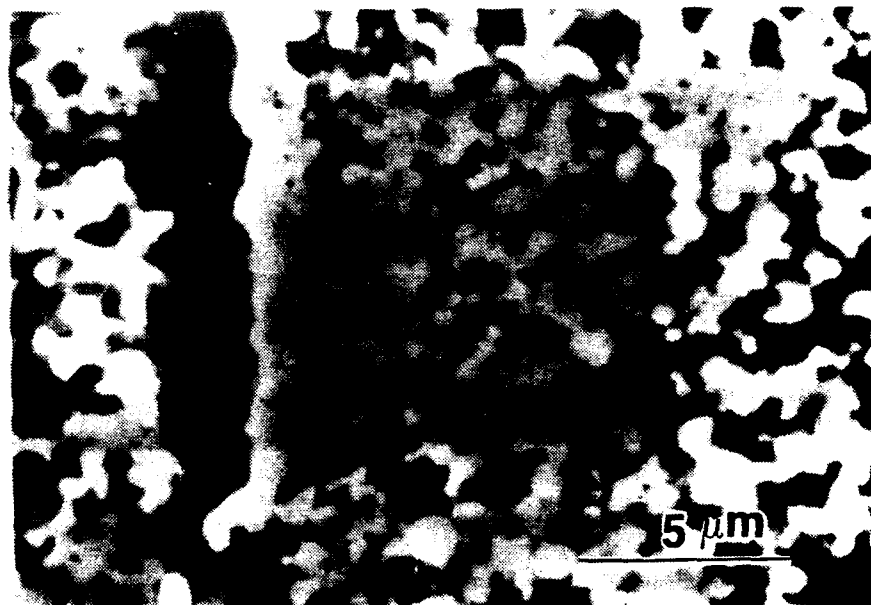
Figure 19. Backscattered SEM micrograph showing the
beginning of the reaction zone. EDX analysis
showed that the lighter phase (high Z) is
mostly ZrO_2 and the dark phase (lower Z) is
mostly YVO_4. Same sample as in figure 18.

On going inland from the exposed surface, near the
center of the reaction zone, these regions, the light and dark
phases, become more narrow (1-2 μm across); thus overlap
from neighboring regions decreases the accuracy of the EDX
results. Figure 20 is a blow up of the middle of the reaction

zone showing the finer regions of the light and dark phases compared with the start of the zone.
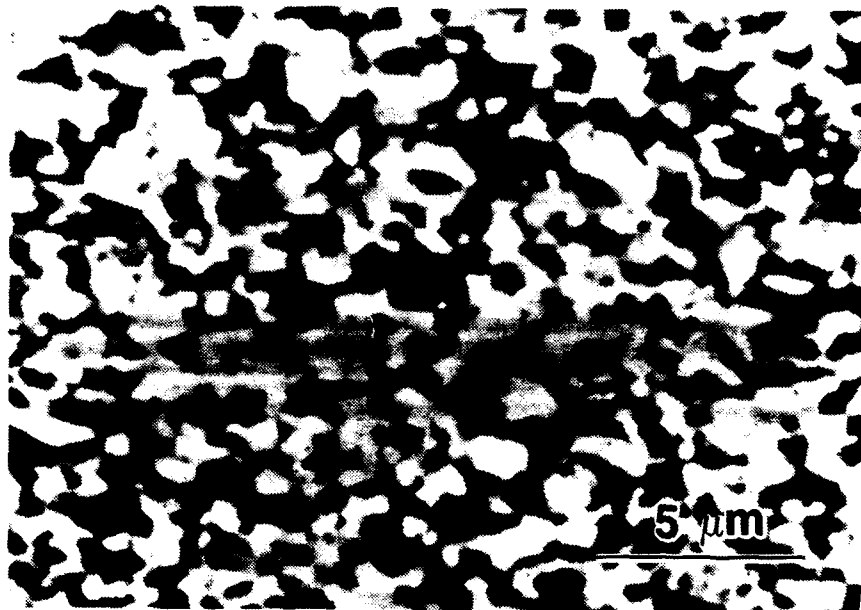
Figure 20. Middle of the reaction zone. Backscattered SEM micrograph on the same sample as in figure 18.

The segregation appears to extend all across the reaction zone, and near the end of the zone this is on a much finer scale (unresolvable with SEM). EDX analysis now cannot to be performed because the phases are separated by distances that are much smaller than the limit of spatial resolution for the EDX. Figure 21 shows very clearly the finer scale of the two phases compared with the middle of the reaction zone.
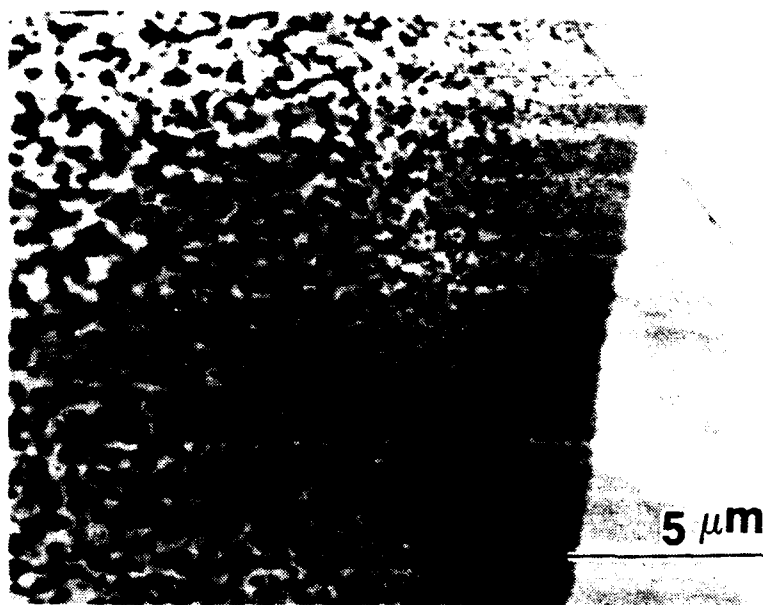
Figure 21. End of the reaction zone. Backscattered SEM micrograph showing the two phases to be present on a much finer scale as we go towards the end of the reaction zone. Same sample as on figure 18.

Further TEM studies with EDX analysis are necessary to fully characterize these regions at the center of the zone and near the end of it. The matrix composition of the unreacted YSZ single crystal was found to be, by EDX analysis, 19.4% weight of Y_2O_3 (specimen YSZ-20%wt Y_2O_3). This suggests that the NPS EDX was well calibrated and the results are accurate as long as data are taken well above the limit of resolution.

v. CONCLUSIONS

From an analysis of the results of the experiments on both the powder samples and the single crystals using XRD, TEM, and SEM, the following conclusions can be drawn.

First, the ZrO_2 reacts slowly with small amounts of V_2O_5 at 900°C in air, to form either (a) a glassy phase or (b) a solid solution. The valency of V adopted in this reaction is not clear.

Secondly the cubic and tetragonal YSZ react with V_2O_5 to form YVO_4 and monoclinic ZrO_2, and that this segregation in single crystal samples appears to extend all across the reaction zone.

VI. RECOMMENDATIONS

The reaction between YSZ and V_2O_5 seems to be well established, but the nature of the segregation between the ZrO_2 and YVO_4 regions is not yet understood at the center and end of the reaction zones in single crystal samples. In order to fully characterize these regions it is necessary to perform TEM studies with EDX analysis on the reaction zones in YSZ single crystals exposed to V_2O_5 melts.

Another suggestion for further work is an investigation to try and fully understand the reaction between the ZrO_2 and V_2O_5. TEM studies on pure ZrO_2 single crystals exposed to V_2O_5 melts are recommended to achieve this.

LIST OF REFERENCES

1. E.C. Subbarao, in A.H. Heuer and L.W. Hobbs (eds.), *Science and Technology of Zirconia, Advances in Ceramics*, Vol. 3, pp.1-24, American Ceramic Society, Columbus, OH, 1981.

2. D.W. Susnitzky, W. Hertl, and a C. Barry Carter, "Destabilization of Zirconia Thermal Barriers in the Presence of V_2O_5", *Journal of the American Ceramic Society*, Vol.71, No.11, pp. 992-1004, 1988.

3. W.M. Kriven, W.L. Fraser, and S.W. Kennedy, in A.H. Heuer and L.W. Hobbs (eds.), *Science and Technology of Zirconia, Advances in Ceramics*, Vol. 3, pp. 82-97, American Ceramic Society, Columbus, OH, 1981.

4. V.S. Stubican, R.C. Hink, and S.P. Ray, *Journal of the American Ceramic Society*, Vol.61, No.1-2, pp. 17-21, 1978.

5. V.S. Stubican, and J.R. Hellmann, in A.H. Heuer and L.W. Hobbs (eds.), *Science and Technology of Zirconia, Advances in Ceramics*, Vol. 3, pp. 25-36, American Ceramic Society, Columbus, OH, 1981.

6. A.H. Heuer, R. Chaim, and V. Lanteri, "Review: Phase Transformations and Microstructural Caracterization of Alloys in the System Y_2O_3-ZrO_2", *Advances in Ceramics*, Vol. 24, *Science and Technology of Zirconia III*, The American Ceramic Society, Inc., 1988.

7. R.L. Jones, C.E. Williams, and S.R. Jones, "Reaction of Vanadium Compounds with Ceramic Oxides", *Journal of the Electrochemical Society*, Vol.133, No.1, pp. 227-230, Jan 1986.

8. R.L. Jones and C.E. Williams, "Hot Corrosion Studies of Zirconia Ceramics, *Surface and Coating Technology*, Vol.32, pp. 349-358, 1987.

9. R.L. Jones, "The Development of Hot Corrosion-resistant Zirconia Thermal Barrier Coating", *Materials at High Temperatures*, Vol.9, No.4, pp. 228-236, 1991.

10. J.S. Patton, J. Hellman, and W.R. Bitler, "Thermochemical Stability of Whisker Reinforced/Thermal Barrier Coatings in Corrosive Combustion Ambients", *Technical Report to Office of Naval Research,* C: N00014-90-J-1145, 1992.

11. C.F. Grain, *Journal of the American Ceramic Society,* Vol.50, No.6, pp. 289, 1967.

12. R.C. Buchanan, and G.W. Walter,*Journal of the Electrochemical Society,* Vol.130, p. 1905, 1983.

13. Vittorio Cirilli, Aurelio Burdese, and Cesare Brisi, *Atti Accad. Sci. Torino,* Vol.95, p. 14, 1961.

14. E.M. Levin, *Journal of the American Ceramic Society,* Vol.50, No.7, p. 381, 1967.

15. A.A. Fotiev and V.L. Volkov, *Zh. Fiz. Khim.,* Vol.45, No.10, p. 2671, 1971.

16. Yungshon Hon and Puayan Shen, "Phase Transformations of (Ca,Ti) Partially Stabilized Zirconia", *Materials Science and Engineering,* Vol.A131, pp. 273-280, 1991.

17. P.R. Krishnamoorthy, Parvati Ramaswamy, B.H. Narayana, "Microstructural Developments in Mg-Ti-PSZ", *Journal of Materials Science,* Vol.27, pp. 1016-1022, 1992

18. R.L. Bratton and S.K. Lau, in A.H. Heuer and L.W. Hobbs (eds.), *Science and Technology of Zirconia, Advances in Ceramics,* Vol. 3, p. 226, American Ceramic Society, Columbus, OH, 1981.

19. M.H. Loretto,"Electron Beam Analysis of Materials", *Chapman and Hall Ltd,* 1984.

20. V.I. Matkovitch and P.M. Corbett, "Formation of Zircon from Zirconium Dioxide and Silicon Dioxide in the Presence of Vanadium Pentoxide", *Journal of the American Ceramic Society,* Vol.44, No.3, p. 128, 1961.

INITIAL DISTRIBUTION LIST

		No. Copies
1.	Deffense Technical Information Center Cameron Station Alexandria, VA 22304-6145	2
2.	Library, Code 52 Naval Postgraduate School Monterey, CA 93943-5002	2
3.	Naval Engineering Curricular Office, Code 34 Naval Postgraduate School Monterey, CA 93943-5100	1
4.	Prof. M. D. Kelleher, Code ME/Kk Chairman Department of Mechanical Engineering Naval Postgraduate School Monterey, CA 93943-5100	1
5.	Prof. A. G. Fox, Code ME/Fx Department of Mechanical Engineering Naval Postgraduate School Monterey, CA 93943-5100	2
6.	Embassy of Greece Naval Attache 2228 Massachusetts Ave., N.W. Washington, D.C. 20008	3
7.	Mr. Joel S. Patton, Code 2813 Naval Surface Warfare Center Annapolis Detachment of the Carderock Division Annapolis, Maryland 21402	1
8.	LT Konstandinos Kondos Knossou 4 Patisia 11253 Athens, Greece	3